Supporting Information for

Antitumor Potential of the Isoflavonoids (+)- and (–)-2,3,9-Trimethoxypterocarpan: Mechanism-of-Action Studies

Kaio Farias,[a] Roner F. da Costa,[b] Assuero S. Meira,[a] Jairo Diniz-Filho,[a] Eveline M. Bezerra,[b] Valder N. Freire,[c] Prue Guest,[d] Maryam Nikahd,[d] Xinghua Ma,[d] Michael G. Gardiner,[d] Martin G. Banwell,[d,e,*] Maria da C. F. de Oliveira,[f] Manoel O. de Moraes,[a] and Claudia do Ó. Pessoa[a,*]

[a] Department of Physiology and Pharmacology, Faculty of Medicine, Federal University of Ceará, Fortaleza, CE, 60430-275, Brazil.

[b] Department of Natural Sciences, Mathematics and Statistics, Federal Rural University of the Semi-Arid Region - UFERSA, Mossoró - RN, Brazil.

[c] Department of Physics, Science Center, Federal University of Ceará, Fortaleza, CE, 60430-275, Brazil.

[d] Research School of Chemistry, Institute of Advanced Studies, The Australian National University, Canberra, ACT 2601, Australia.

[e] Institute for Advanced and Applied Chemical Synthesis, Jinan University, Guangzhou, 510632, China.

[f] Department of Organic and Inorganic Chemistry, Science Center, Federal University of Ceará, Fortaleza, CE, 60430-275, Brazil.

Contents

Contents (contd)

Chemical Synthesis Studies

Outline of Chemical Synthesis Studies

The first synthesis of compound (±)-**1** was reported in 1967,[1] almost a decade before the identification of (–)-**1** as a natural product.[2] In 2016, and in the only other synthesis reported thus far, an intermolecular Mizoroki-Heck oxyarylation reaction[3,4] involving 6,7-dimethoxy-2*H*-chromene and 2-iodo-5-methoxyphenol as substrates provided compound (±)-**1** in a direct but rather inefficient manner.[5] This strategy has been exploited in the synthesis of a range of analogues, some of which were obtained in slightly enantiomerically-enriched form.[6] The route used (Scheme S1) to obtain compound (±)-**1** as part of the present study followed the same lines and started with subjection of the known[7] and readily available aryl propargyl ether **2** to a gold(I)-catalyzed intramolecular hydroarylation reaction.[8,9] When the commercially available catalyst JohnPhosAu(acetonitrile)hexafluoroantimonate was used a rather inefficient reaction took place to deliver a mixture of the isomeric and known cyclization products **3** (6%)[8] and **4** (9%)[8] together with the previously reported[9] and formal [2+2]-dimer **5** (3%) of the latter. These three products were separated using conventional chromatographic techniques and the structure of cyclobutane **5** was confirmed by single-crystal X-ray analysis (See Supporting Information - SI - for details). Higher yields (up to 40%) of the desired 2*H*-chromene **4** were obtained by variations of these conditions[8] but this was still accompanied by isomer **3** (13%). Stratakis and co-workers have reported[10] that by using $Ph_3PAuNTf_2$ as the catalyst in the same reaction the yields of product **4** could be raised to 97%. In keeping with earlier approaches to the pterocarpans,[3-6] an equimolar mixture of compound **4** and the commercially available phenol **6** was subjected to a Mizoroki-Heck oxyarylation reaction using a combination of $Pd(OAc)_2$ and silver carbonate in the presence of the bidentate ligand 1,2-bis(diphenylphosphino)ethane (dppe) and thereby affording, after chromatographic purification, (±)-2,3,9-trimethoxypterocarpan [(±)-**1**] in 43% yield. All of the spectral data acquired on this compound matched those reported for the corresponding natural product.[2] Various attempts were made to increase the yield of product (±)-**1** from this reaction but

to no avail and with the balance of the material appearing to be oligomeric in nature. As detailed below, the racemate was resolved into the constituent enantiomers using semi-preparative chiral HPLC techniques. The more mobile enantiomer was the (–)-form and this is presumed, based on earlier studies,[2] to possess the *R*-configuration at both C6a and C11a. Consistent with this assumption, a single-crystal X-ray analysis of the (+)-enantiomer (see SI for details) established it was the 6a*S*, 11a*S*-configured material.

Scheme S1. The protocols used in the present study to prepare (±)-2,3,9-trimethoxypterocarpan [(±)-**1**] and then separate the constituent enantiomers.

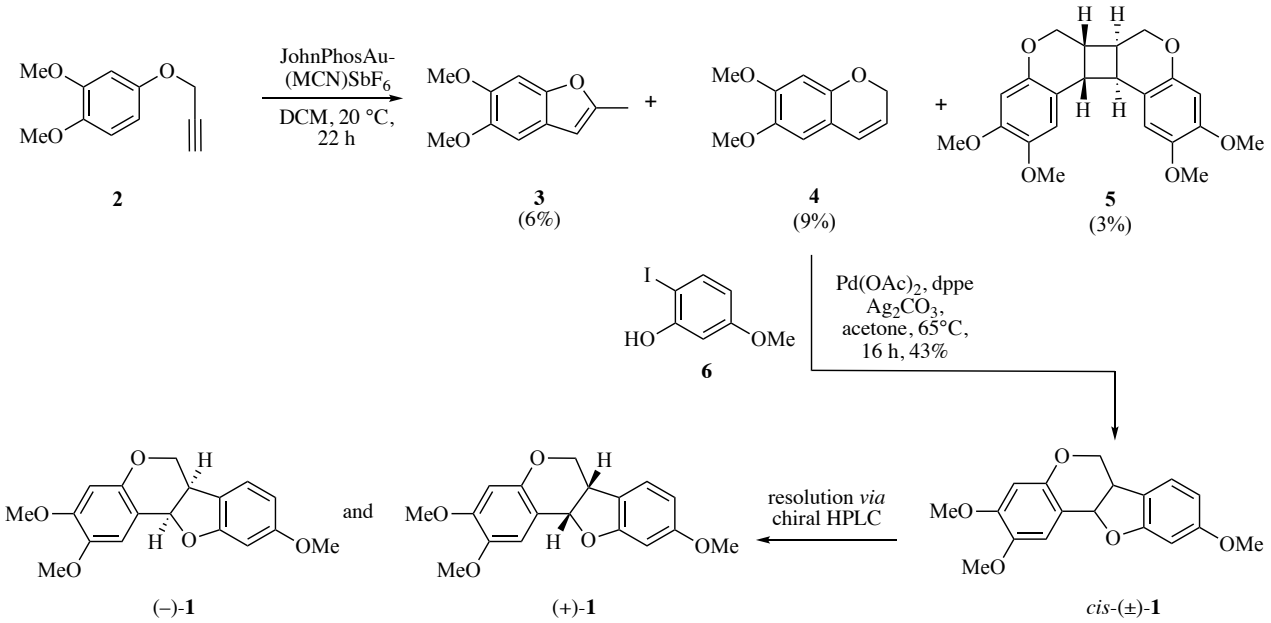

General Procedures for Chemical Synthesis Studies

Unless otherwise specified, proton (^{1}H) and proton-decoupled carbon [^{13}C{^{1}H}] NMR spectra were recorded at room temperature in base-filtered $CDCl_3$ on a Varian spectrometer operating at 400 MHz for proton and 100 MHz for carbon nuclei. For ^{1}H NMR spectra, signals arising from the residual protio-forms of the solvent were used as the internal standards. ^{1}H NMR data are recorded as follows: chemical shift (δ) [multiplicity, coupling constant(s) *J* (Hz), relative integral] where multiplicity is defined as: s = singlet; d = doublet; t = triplet; q = quartet; m = multiplet or combinations of the above. The signal due to residual $CHCl_3$ appearing at δ_H 7.26 and the central resonance of the $CDCl_3$ "triplet" appearing at δ_C 77.16 were used to reference ^{1}H and ^{13}C{^{1}H} NMR spectra, respectively. Infrared spectra (ν_{max}) were recorded on a Perkin–Elmer 1800 Series FTIR Spectrometer. Samples were analyzed as thin films. Low-resolution ESI mass spectra were recorded on a single quadrupole liquid chromatograph-mass spectrometer, while high-resolution measurements were conducted on a time-of-flight instrument. Low- and high-resolution EI mass spectra were recorded on a magnetic-sector machine. Melting points were measured on a Reichert melting point microscope and are uncorrected. Analytical thin layer chromatography (TLC) was performed on aluminum-backed 0.2 mm thick silica gel 60 F_{254} plates as supplied by Merck. Eluted plates were visualized using a 254 nm UV lamp and/or by treatment with a suitable dip followed by heating. These dips included phosphomolybdic acid : ceric sulfate : sulfuric acid (conc.) : water (37.5 g : 7.5 g : 37.5 g : 720 mL) or potassium permanganate : potassium carbonate : 5% sodium hydroxide aqueous solution : water (3 g : 20 g: 5 mL : 300 mL). Flash chromatographic separations were carried out following protocols defined by Still *et al.*[11] with silica gel 60 (40–63 μm) as the stationary phase and using the AR- or HPLC-grade solvents indicated. Starting materials and reagents were generally available from the Sigma–Aldrich, Merck, TCI, Strem or Lancaster Chemical Companies and were used as supplied. Drying agents and other inorganic salts were purchased from the AJAX, BDH or Unilab Chemical Companies. Tetrahydrofuran (THF), methanol and dichloromethane were dried using a Glass Contour solvent purification system that is based upon a technology originally described by Grubbs *et al.*[12] Petroleum ether refers to the fraction boiling between 40 and 60 °C. Where necessary, reactions were performed under a nitrogen atmosphere.

Specific Procedures for Chemical Synthesis Studies

*Synthesis of Compound **2***

A magnetically stirred solution of 3,4-dimethoxyphenol (3.08 g, 20.0 mmol) in DMF (100 mL) maintained under a nitrogen atmosphere at 20 °C was treated, dropwise, with propargyl bromide (3.57 g of an 80 wt % solution in toluene, 24.0 mmol) then anhydrous K_2CO_3 (3.32 g, 24.0 mmol). The ensuing mixture was stirred at ambient temperatures for 22 h before being quenched with NH_4Cl (150 mL of a saturated aqueous solution) and extracted with diethyl ether (3 x 100 mL). The combined organic phases were washed with brine (2 x 100 mL) before being dried ($MgSO_4$), filtered and concentrated under reduced pressure. The residue thus obtained was dissolved in CH_2Cl_2/hexane (5 mL of a 1:1 v/v mixture) and the resulting solution passed through thin pad of TLC-grade silica gel contained in a sintered glass funnel. The pad was washed with CH_2Cl_2/hexane (20 mL of a 1:1 v/v mixture) and the combined filtrates concentrated under reduced pressure to afford compound **2** (3.47 g, 90%) as a clear, light-yellow oil. This material was identical, in all respects, with that obtained previously.[7,8]

*The Gold(I)-Catalyzed Intramolecular Hydroarylation Reaction of Compound **2**. Formation of Benzofuran **3**, 2H-Chromene **4** and the 2H-Chromene Dimer **5**.*

A magnetically stirred solution of propargyl ether **2** (300 mg, 1.56 mmol) in dichloromethane (10 mL) maintained at 20 °C under an atmosphere of nitrogen was treated with JohnPhosAu(acetonitrile)hexafluoroantimonate (7.72 mg, 0.01 mmol). The ensuing mixture was stirred at ambient temperatures for 16 h then concentrated under reduced pressure and the dark-green residue so-obtained subjected to flash chromatography (silica, 0:10 → 4:6 v/v ethyl acetate/petroleum ether gradient elution) to give three fractions, A B and C.

Concentration of fraction A (R_f = 0.8 in 4:94 v/v ethyl acetate/petroleum ether) afforded compound **4** (29.4 mg, 9%) as a clear, colorless oil and that was identical, in all respects, with that obtained previously.[8]

Concentration of fraction B (R_f = 0.8 in 3:7 v/v ethyl acetate/petroleum ether) afforded compound **3** (17.8 mg, 6%) as a clear, colorless oil and that was identical, in all respects, with that obtained previously.[8]

Concentration of fraction C (R_f = 0.4 in 2:3 v/v ethyl acetate/petroleum spirit) afforded compound **5**[9] (14.5 mg, 3%) as a white, crystalline solid, m.p. = 219-224. ^{1}H NMR (400 MHz, $CDCl_3$) δ 6.57 (s, 2H), 6.43 (s, 2H), 4.13 (m, 2H), 3.85 (s, 6H), 3.83 (s, 6H), 3.75 (m, 2H), 3.00 (m, 4H). $^{13}C\{^1H\}$ NMR (100 MHz, $CDCl_3$) δ 149.1, 148.7, 144.5, 117.7, 112.5, 102.0, 66.2, 57.0, 56.1, 40.7, 33.2. IR ν_{max} (KBr) 2949, 2933, 1616, 1507, 1461, 1263, 1221, 1191, 1173, 1125,

1019, 944, 856 cm^{-1}. HRMS (ESI, +ve) calcd for $C_{44}H_{48}O_{12}Na$ [$(2M + Na)^+$] 791.3043, found 791.3043.

*Synthesis of (±)-2,3,9-Trimethoxypterocarpan [(±)-**1**]*

bis-(Diphenylphosphino)ethane (dppe) (462 mg, 1.160 mmol) was added to a magnetically stirred solution of palladium acetate (130 mg, 0.579 mmol) in acetone (120 mL) maintained under a nitrogen atmosphere at 20 °C. The ensuing mixture was stirred at 70 °C for 0.66 h then treated with commercially available compound **6** (2.0 g, 8.00 mmol). After a further 0.25 h Ag_2CO_3 (2.15 g, 7.80 mmol) and compound **5** (743 mg, 3.865 mmol) were added to the reaction mixture and after a further 48 h (at 70 °C) the reaction mixture was cooled to 20 °C then filtered through a short pad of TLC-grade silica gel contained in a sintered-glass funnel. The filtrate was concentrated under reduced pressure and the residue so-obtained was subjected to flash chromatography (silica, 1:5 v/v ethyl acetate/hexane elution) to give, after concentration of the appropriate fractions (R_f = 0.3 in 1:2.5:5.5 v/v/v ethyl acetate/CH_2Cl_2/hexane), compound (±)-**1** (518 mg, 43%) as a white, crystalline solid, m.p. = 115-118 °C (lit.[1] m.p. = 122-123 °C). ^{1}H NMR (400 MHz, $CDCl_3$) δ see Table S1. $^{13}C\{^1H\}$ NMR (100 MHz, $CDCl_3$) δ see Table S2. IR ν_{max} (neat) 3435, 3063, 2998, 2938, 2869, 2835, 1620, 1598, 1513, 1496, 1465, 1447, 1419, 1385, 1345, 1332, 1304, 1269, 1221, 1210, 1194, 1176, 1146, 1134, 1085, 1030, 990, 949, 902, 848, 832, 774, 757, 730, 705, 730 cm^{-1}. HRMS (EI, 70 eV) calcd for $C_{18}H_{18}O_5$ ($M^{+\bullet}$) 314.1154, found 314.1151.

Where valid comparisons could be made (see below) the ^{1}H NMR, ^{13}C NMR and IR spectroscopic data as well and the MS spectral data recorded on this material compared favorably with those reported for the naturally occurring (–)-enantiomer[2] and/or the racemate.[5]

*Chromatographic Resolution of Compound (±)-**1** and Characterization of the Separated Enantiomers (+)-**1** and (–)-**1***

A sample of (±)-2,3,9-trimethoxypterocarpan [(±)-**1**, 113 mg] was subjected to chiral HPLC on a Daicel CHIRALPAK®IA Semi-Prep column (250 mm x 20 mm, 5 μm particle size – Part Number 80345) using 7:3 v/v *i*-PrOH/hexane as the eluting solvent at a flow rate of 8 mL/min. Baseline separation of two fractions, A and B, was thus achieved.

Concentration of fraction A (R_t 15.7 min) afforded compound (–)-**1** (43.3 mg) as a clear, colorless oil, $[\alpha]_D$ = –253° (*c* 1.0, ethanol) {lit.[2] $[\alpha]_D$ = –228° (ethanol)}. The NMR, IR and MS spectral data acquired on this material matched those recorded on the racemate (±)-**1**.

Concentration of fraction B (R_t 20.2 min) afforded compound (+)-**1** (48.6 mg) as a clear, colorless oil, $[\alpha]_D$ = +203° (*c* 1.3, ethanol) {lit.[13] $[\alpha]_D$ = +266° (*c* 0.001, ethanol)}. The NMR, IR

and MS spectral data acquired on this material matched those recorded on the racemate (±)-**1**. A crystal of compound (+)-**1** suitable for single-crystal X-ray analysis could be grown from methanol.

***Table S1**: Comparison of the [1]H NMR Data Reported[2] for the Natural Product (–)-**1** with those Obtained on the Synthetically-derived Racemate (±)-**1**.*

δ_H (–)-**1**[a,b]	δ_H (±)-**1**[c,b]	δ_H (±)-**1**[e,f]
not reported	3.53 (m, 1H)	3.48-3.57 (m, 1H)
not reported	3.59 (t, *J* = 10.8 Hz, 1H)	3.59 (t, *J* = 11.4 Hz, 1H)
3.78 (s, 3H)	3.77 (s, 3H)	3.76 (s, 3H)
3.86 (s, 3H)	3.86 (s, 3H)	3.85 (s, 3H)
3.91 (s, 3H)	3.90 (s, 3H)	3.89 (s, 3H)
not reported	4.24 (m, 1H)	4.23 (dd, *J* = 10.1 and 4.1 Hz, 1H)
not reported	5.49 (d, *J* = 6.8 Hz, 1H)	5.48 (d, *J* = 6.4 Hz, 1H)
6.44 (q, *J* = 8.8 and 2.5 Hz, 1H) and 6.45 (d, *J* = 2.5 Hz, 1H)	6.45 (m, 2H)	6.44-6.46 (m, 2H)
6.47 (s, 1H)	6.49 (s, 1H)	6.48 (s, 1H)
6.97 (s, 1H)	6.98 (s, 1H)	6.97 (s, 1H)
7.12 (d, *J* = 8.8 Hz, 1H)	7.13 (d, *J* = 9.2 Hz, 1H)	7.12 (d, *J* = 9.2 Hz, 1H)

[a]data derived from reference 2; [b]spectrum recorded at 90 MHz in $CDCl_3$; [c]compound prepared during the current study; [d]spectrum recorded at 100 MHz in $CDCl_3$; [e]data derived from reference 5; [f]spectrum recorded at 100 MHz in $CDCl_3$.

***Table S2**: Comparison of the ^{13}C NMR Data Derived from the Racemate (±)-**1** with Those Reported by Kakuda* et al.[5]

δ_C (±)-**1**[a,b]	δ_C (±)-**1**[c,b]	$\Delta\delta_C$
39.8 (CH)	39.8	0
55.6 (CH_3)	55.6	0
56.0 (CH_3)	56.0	0
56.4 (CH_3)	56.4	0
66.8 (CH_2)	66.8	0
78.9 (CH)	77.5	1.4
97.0 (CH)	97.0	0
100.9 (CH)	100.9	0
106.4 (CH)	106.4	0
110.7 (C)	110.7	0
112.3 (CH)	112.3	0
119.2 (C)	119.2	0
124.9 (CH)	124.9	0
144.4 (C)	144.4	0
150.0 (C)	150.0	0
150.7 (C)	150.6	0.1
160.7 (C)	160.7	0
161.2 (C)	161.2	0

[a]data derived from compound (±)-**1** prepared during the current study; [b]spectrum recorded at 100 MHz in $CDCl_3$; [c] data derived from reference 5; [d]spectrum recorded at 100 MHz in $CDCl_3$.

Crystallographic Studies

Crystallographic Data.

Compound (+)-**1**. $C_{18}H_{18}O_5$, M = 314.32, T = 150 K, monoclinic, space group $P2_1$, Z = 4, a = 4.76720(10) Å, b = 18.8707(4) Å, c = 16.6201(4) Å; α = 90°, β = 93.099(2)°, γ = 90°; V = 1492.96(6) Å^3, D_x = 1.398 Mg m^{-3}, 5951 unique data ($2\theta_{max}$ = 148.23°), R = 0.0390 [for 5716 reflections with $I > 2.0\sigma(I)$]; Rw = 0.1057 (all data), S = 1.038.

Compound **5**. $C_{22}H_{24}O_6$, M = 384.41, T = 150 K, monoclinic, space group $P2_1/c$, Z = 4, a = 16.0596(19) Å, b = 4.9375(7) Å, c = 24.003(3) Å; α = 90°, β = 104.836(12)°, γ = 90°; V = 1839.8(4) Å^3, D_x = 1.388 Mg m^{-3}, 2751 unique data ($2\theta_{max}$ = 122.138°), R = 0.0762 [for 1392 reflections with $I > 2.0\sigma(I)$]; Rw = 0.1877 (all data), S = 1.042.

Structure Determinations.

Data for compounds (+)-**1** and **5** were measured on a Rigaku SuperNova diffractometer using CuKα, graphite monochromator (λ = 1.54184 Å). Data collection, cell refinement and data reduction employed the CrysAlis PRO program[14] while SHELXT[15] and SHELXL[16] were used for structure solution and refinement. Atomic coordinates, bond lengths and angles, and displacement parameters have been deposited at the Cambridge Crystallographic Data Centre (CCDC no. 1984031). These data can be obtained free-of-charge via www.ccdc.cam.ac.uk/data_request/cif, by emailing data_request@ccdc.cam.ac.uk, or by contacting The Cambridge Crystallographic Data Centre, 12 Union Road, Cambridge CB2 1EZ, UK; fax: +44 1223 336033.

Accession Codes

CCDC depositions 1984031 and 1985403 contains the supplementary crystallographic data for this paper. These data can be obtained free of charge via www.ccdc.cam.ac.uk/data_request/cif, or by e-mailing data_request@ccdc.cam.ac.uk, or by contacting The Cambridge Crystallographic Data Centre, 12 Union Road, Cambridge CB2 1EZ, U.K.; fax: +44 1223 336033.

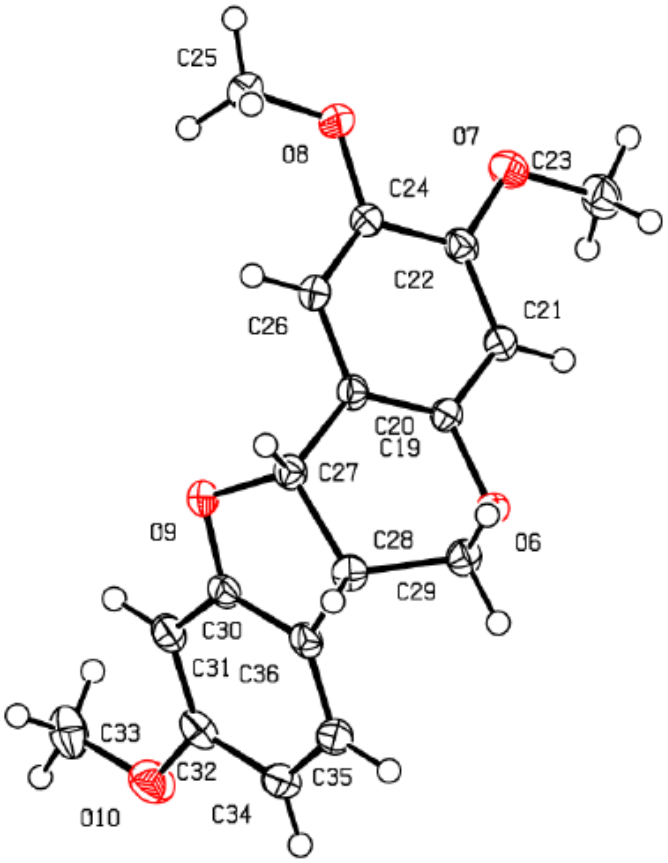

Figure S1: Structure of compound **(+)-1** (CCDC 1985403). Anisotropic displacement ellipsoids show 30% probability levels. Hydrogen atoms are drawn as circles with small radii (crystal grown from methanol).

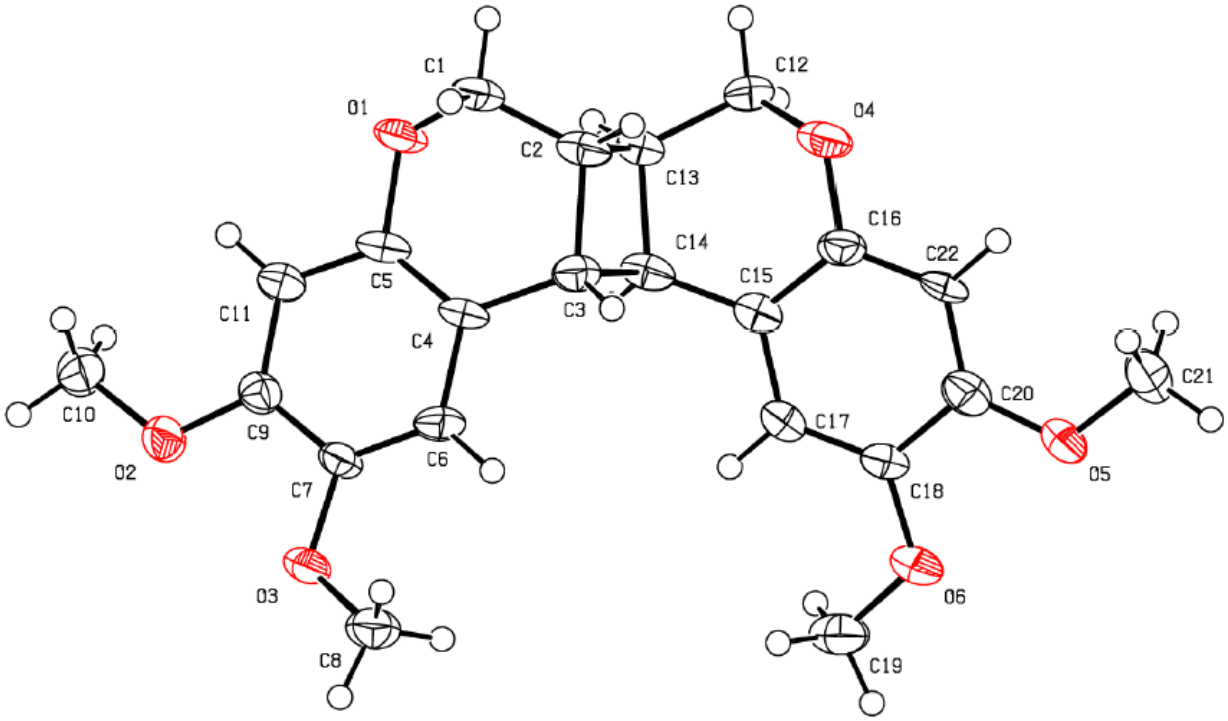

Figure S2: Structure of compound **5** (CCDC 1984031) Anisotropic displacement ellipsoids show 30% probability levels. Hydrogen atoms are drawn as circles with small radii (crystal grown from methanol).

Biological Studies

Cell Lines

The four human cancer cell lines used in the present study were obtained from the National Cancer Institute (Bethesda, MD, USA), these being HL-60 (promyelocytic leukemia), HCT-116 (colon), OVCAR-8 (ovarian adenocarcinoma) and SF-295 (glyoblastoma). The cells were maintained in RPMI 1640 medium supplemented with 10% fetal bovine serum, 2 mM glutamine, 100 U/mL penicillin and 100 μg/mL streptomycin at 37 °C under a 5% CO_2 atmosphere.

MTT Cell Viability Assays

Cells were plated onto 96-well plates (0.1-0.7 × 10^6 cells/mL) then a solution of the test compound in DMSO added to the individual wells. In the case of the controls, the same amount of vehicle (DMSO) alone was used. The plate thus prepared was incubated at 37 °C under a 5% CO_2 atmosphere. After incubation periods of 24, 48 and 72 h the supernatant within each well was replaced by fresh medium containing MTT (0.5 mg/mL) and the system agitated for a further 3 h before the MTT formazan product was dissolved in DMSO (150 μL) and absorbance of the resulting solution was measured at 595 nm (using a Beckman Coulter DTX-880 Multimode Detector). The final concentration of DMSO in the culture medium was kept constant and below 0.1% v/v. All cell treatments were carried out in triplicate.

Morphological Analyses Using Fluorescence Microscopy

Acridine orange/ethidium bromide (AO/EB) stainings of OVCA-8 cells were performed to determine the cell death pattern induced by increasing concentrations of compound (+)-**1**. While AO and EB are DNA intercalating molecules, the first is still able to cross intact membranes and confers a green hue to the nuclei of viable cells. EB, on the other hand, is mainly incorporated by non-viable cells, notably when cell membranes are unstable, and so staining the associated nuclei red.[17] So, after 48 h of incubation, the cells were trypsinized, centrifuged and resuspended in phosphate-buffered saline (PBS, pH 7.4) solution. A 50 μL aliquot of cell suspension was removed and transferred to another tube (tube A). A solution containing 8 μL of PBS, 2 μL of acridine orange (100 μg/mL) and 10 μL of EB (20 μg/mL) was prepared in a second tube. Next, 1 μL of this latter solution was added to the contents of tube A containing the 50 μL aliquot of suspended cells. Thereafter, the cells were counted and classified using a fluorescence microscope (Olympus, Tokyo, Japan). Three hundred cells were counted per sample and categorized as follows: viable cells, apoptotic cells and necrotic cells.

Analysis of Changes in Cell Morphology

Untreated OVCAR-8 cells as well as those treated with compound (±)-**1** were examined for morphological changes using light microscopy (Olympus, Tokyo, Japan). In order to evaluate nuclear morphology, cells were harvested, transferred to cytospin slides, fixed with methanol for 1 min. then stained with hematoxylin-eosin (H&E, Sigma Aldrich Co., St. Louis, MO/USA) using established protocols.[18] Paclitaxel (PTX, 0.03 μM) was used as the positive control.

Cell Proliferation Assays Conducted Using the xCELLigence Biosensor System

Experiments were carried out using the the xCELLigence system (Roche Diagnostics, QC) incorporating a Real-Time Cell Analyzer (RTCA)/Dual-Plate (DP) Facility. Supplier-defined protocols were followed in every instance. Thus, the optimal cell concentrations for the proliferation assays were first determined and then OVCAR-8 cells were seeded at 5000 cells/well in complete medium (200 μL) using an E-plate insert 16 (Roche Diagnostics) specifically designed for ready measurement of cellular impedance and incubated for 72 h at 37 °C under a humidified atmosphere containing 5% CO_2 and after which time the test substrate was added (and this defined as T = O hour in Figure 2). In such experiments, OVCAR-8 cells were used to test the cytotoxicity of compounds (±)-**1** and (+)-**1** at concentrations of 1.0, 2.0 and 4.0 μM. Paclitaxel (PTX) was used, at a concentration of 0.5 μM, as the positive control and impedance values are expressed as an arbitrary unit called the Cell Index. Each such experiment was performed in duplicate wells.

Cell Cycle Analyses

OVCAR-8 cells were treated with compound (±)-**1** (5.0 and 10.0 μM), compound (+)-**1** (2.5, 5.0 and 10.0 μM) or paclitaxel (PTX) (0.05 μM) for 24 h. Harvested cells were incubated, away from light, at 25 °C for 0.5 h in a lysis buffer solution containing 0.1% sodium citrate, 0.1% Triton X-100 and 75 μM propidium iodide. The resulting cells were then analyzed by flow cytometry on an EasyCyte System (Guava Technologies Inc.). Five thousand events were evaluated per sample, and cellular debris was omitted from the analysis. Paclitaxel (PTX) (0.05 μM) was used as the positive control.

Statistical Analyses

The obtained data are presented as the means ± standard deviation (SD) from n experiments. ANOVA and the Dunnet's test were used to compare mitotic phase data and to measure changes in cell viability. The significance level was set at 5%.

Theoretical Studies

Docking

The molecular docking of (+)-2,3,9-trimethoxypterocarpan [(+)-**1**] into kinesin Eg5 (pdb entry 1X88) was carried out using Version 4.0 of the suite of Autodock tools. The AutoDockTools (ADT) interface[19] was used for checking molecular models, adding hydrogen atoms, as well as for polar hydrogen merging, for introducing partial (Gasteiger) charges and atom typing assignments. The same interface was used to generate files with appropriate parameters and to analyze results. The parameters for protein solvation and for ligand torsions were both set at the outset while those for the construction of affinity maps [with one map being created for each atom present in compound (+)-**1**] were assigned through a consideration of relevant probe points in a tridimensional grid. The dimensions for this grid were 46.6 × 46.6 × 46.6 Å with probe points separated by 0.8 Å intervals. Consequently, all protein structure models were considered for initial affinity map calculations (blind docking). Other parameters were defined by the default settings within the ADT. Thereafter, all affinity maps were constructed using the auto grid component software within ADT. Such affinity maps were the next step of the study, namely an initial conformational search conducted over the whole protein model that was carried out using the tool within the ADT package. For each run, the maximum number of evaluations and docking runs were 250,000 and 50, respectively. Runs were reinitialized 20 times, with the initial position of compound (+)-**1** changed randomly before each started and so giving a total of 50 × 20 or 1000 docking runs. All other docking parameters were set to the default values with the software package. In the second phase of the study, new affinity maps were constructed by considering the relationships between the best poses of the ligand [(+)-**1**] with Arg221 and a corresponding set of grid parameters established. By such means the grid dimensions and the separation between probe points were refined to 15 × 15 × 15 Å and 0.375 Å, respectively. A new conformational search was then performed, with the maximum number of evaluations/run being 2,500,000 and the number of docking runs being 10. Jobs were reinitialized 20 times starting from random positions for the ligand (+)-**1** and so producing an additional 200 docking runs. The protein structure was kept rigid for all tests while the degrees of freedom for the ligand were confined to translational, rotational and bond torsional processes, the possibilities for the last of these being restricted to the default settings in the ADT.

Quantum Biochemical Calculations

Quantum biochemical interaction calculations were carried out for both monastrol (MON, $C_{14}H_{16}N_2O_3S$, PubChem CID 2987927) and compound (+)-**1**. For those involving MON, the data

derived from the X-ray crystallographic study of human kinensin Eg5 co-crystallized with monastrol were used (pdb entry 1X88, see Figure S3). In case of compound (+)-**1**, the best docking pose as determined above was used. Prior to undertaking the quantum biochemical interaction calculations, the hydrogen atoms were added to both ligands and an optimization procedure then executed using the CHARMM force field.[20] During these optimizations the hydrogen atoms associated with MON were free to move but the co-ordinates of all other atom coordinates were constrained. In contrast, for ligand (+)-**1** all non-hydrogen atoms were also free to move. Quantum level protocols were then used to compute the interaction energies of the ligands with each amino-acid detected in the binding site. An interaction distance, r, of up to 16 Å around from ligands was defined and the associated energies calculated using the Molecular Fragmentation with Conjugated Caps (MFCC) technique.[21-23] This allows for an approximation of the total interaction energy of the full, non-fragmented structure (ligand), through the application of some level of ab initio quantum mechanics in order to solve the Schrödinger equation for parts (fragments) of the ligand-protein complexes. A variant of the MFCC method was implemented locally as Perl scripts. Five neighboring residues (caps) were considered for each side of the amino acid of interest. The interaction (binding) energy E(L − Ri) between the ligand molecule L and the amino acid residue Ri is given by:

$$E(L - Ri) = EA(L + Ri{-}1RiRi{+}1) - EB(Ri{-}1RiRi{+}1) - EC\,(L + Ri{-}1 + Ri{+}1) + ED(Ri{-}1 + Ri{+}1) \quad \ldots(\mathbf{1})$$

where the cap Ri−1 is obtained by attaching a carboxyl or amine group to the dangling bond of the residue Ri. On the right side of equation (**1**) EA(L + Ri−1RiRi+1) is the total energy of the system formed by the ligand and the capped residue; the EB(Ri−1RiRi+1) term is the total energy of the capped residue alone; EC (L + Ri−1 + Ri+1) is the total energy of the system formed by the ligand-molecule and the caps alone. Finally, ED(Ri−1 + Ri+1) is the total energy of the system formed only by the molecular caps. The total binding energy of each ligand was obtained by adding the binding energies with each one of the amino acid residues considered within the chosen binding pocket radius. The energy calculations were performed using the DMol3 program and according to Density Functional Theory (DFT) that employs a local density approximation. The Perdew-Wang (PWC) function[24] was also used and included the dispersion term OBS and Double Numerical plus Polarization (DNP) basis set.

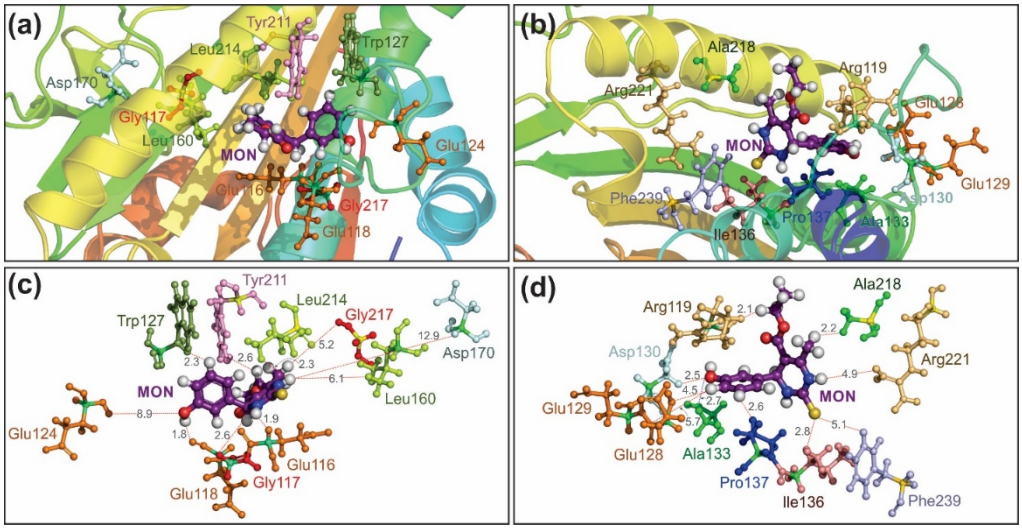

Figure S3. (a and b): the most important amino-acid residues associated with the allosteric binding site of the MON-Eg5 complex. (c and d): key distances between these Eg5 amino-acid residues and the MON ligand (the corresponding interaction energies are the ones making the largest contributions to the total binding energy of the MON-Eg5 complex).

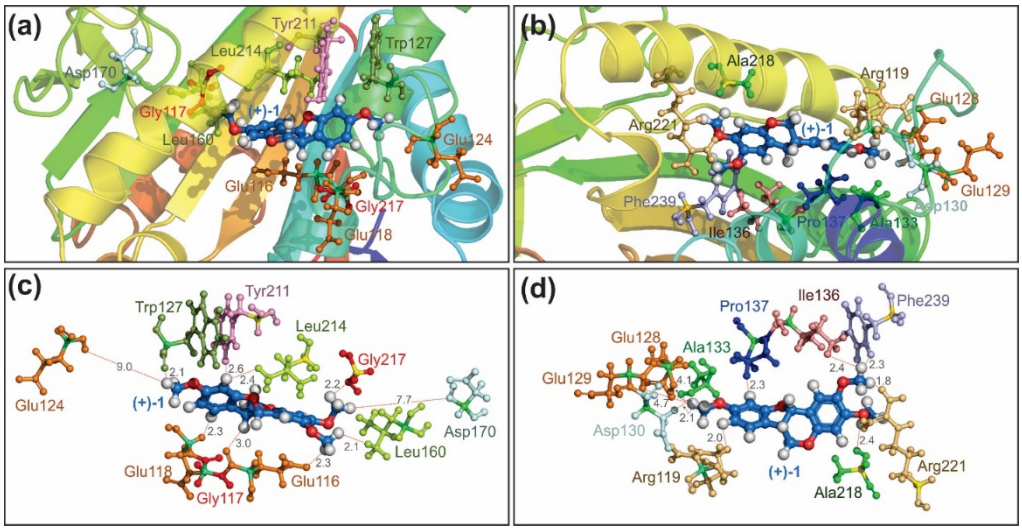

Figure S4. (a and b): the most important amino-acid residues associated with the allosteric binding site of the (+)-**1**-Eg5 complex. (c and d): key distances between these Eg5 amino-acid residues and the (+)-**1** ligand [the corresponding interaction energies are the ones making the largest contributions to the total binding energy of the (+)-**1**-Eg5 complex].

References

1. Kalra, V. K., Kukla, A. S., Seshadri, T. R. Synthesis of new types of pterocarpans. *Ind. J. Chem*. **1967**, *5*(12), 607-9.

2. Pueppke, S. G., VanEtten, H. D. Identification of three new pterocarpans (6a,11a-dihydro-6*H*-benzofuro[3,2-*c*][1]benzopyrans) from *Pisum sativum* infected with *Fusarium solani* f. sp. *pisi*. *J. Chem. Soc., Perkin Trans.* 1, **1975**, 946-8.

3. Kerti, G., Kurtán, T., Antus, S. Study on the reaction mechanism of Heck-oxyarylation of 2*H*-chromenes. *ARKIVOC*, **2009**, (vi), 103-110.

4. Leão, R. A. C., Pinho, V. D., Coelho, A. S., Buarque, C. D., Moraes, P. F., Alonso, D. A., Nájera, C., Costa, P. R. R. Microwave-Promoted Palladium-Catalysed Oxyarylation of Dihydronaphthalene and Chromenes by *o*-Iodophenols and Its Acetates. *Eur. J. Org. Chem*. **2011**, 3313-3316.

5. Kakuda, S., Ninomiya, M., Tanaka, K., Koketsu, M. Synthesis of Pterocarpan Derivatives and their Inhibitory Effects against Microbial Growth and Biofilms. *ChemistrySelect* **2016**, *1*, 4203 – 4208.

6. Kiss, L., Kurtán, T., Antus, S., Brunner, H. Further insight into the mechanism of Heck oxyarylation in the presence of chiral ligands. *ARKIVOC*, **2003**, (v), 69-76.

7. Omokawa, H.; Yamashita, K. Synthesis of (±)-Munduserone via Acetylenic Intermediates. *Agr. Biol. Chem*. **1973**, *37*, 1717-1721.

8. Menon, R. S., Findlay, A. D., Bissember, A. C., Banwell, M. G. The Au(I)-Catalyzed Intramolecular Hydroarylation of Terminal Alkynes Under Mild Conditions: Application to the Synthesis of 2*H*-Chromenes, Coumarins, Benzofurans and Dihydroquinolines. *J. Org. Chem*. **2009**, *74*, 8901-8903.

9. Nevado, C.; Echavarren, A. M. Intramolecular Hydroarylation of Alkynes Catalyzed by Palladium or Gold: Mechanism and *endo*-Selectivity. *Chem. Eur. J*., **2005**, *11*, 3155-3164. The NMR data recorded for dimer **5** in this paper are not in good agreement with our own. The origins of these discrepancies remain unclear.

10. Lykakis, I. N., Efe, C., Gryparis, C., Stratakis, M. $Ph_3PAuNTf_2$ as a Superior Catalyst for the Selective Synthesis of 2*H*-Chromenes: Application to the Concise Synthesis of Benzopyran Natural Products. *Eur. J. Org. Chem*. **2011**, 2334-2338.

11. Still, W. C.; Kahn, M.; Mitra, A. Rapid Chromatographic Technique for Preparative Separations with Moderate Resolution. *J. Org. Chem*., **1978**, *43*, 2923–2925.

12. Pangborn, A. B.; Giardello, M. A.; Grubbs, R. H.; Rosen, R. K.; Timmers, F. J. Safe and Convenient Procedure for Solvent Purification. *Organometallics,* **1996**, *15*, 1518–1520.

13. Militão, G. C., Jimenez, P. C., Wilke, D. V., Pessoa, C., Falcão, M. J. C., Lima, M. A. S., Silveira, E. R., Moraes, M. O., Costa-Lotufo, L. V. (2005). Antimitotic Properties of Pterocarpans Isolated from *Platymiscium floribundum* on Sea Urchin Eggs. *Planta Medica*, **2005**, *71*(7), 683-685.

14. CrysAlis PRO Version 1.171.37.35h (release 09-02-2015 CrysAlis171.NET) (compiled Feb 9 2015,16:26:32) Agilent Technologies: Oxfordshire, UK.

15. Sheldrick, G. M. SHELXT – Integrated Space-Group and Crystal-Structure Determination. *Acta Cryst*. **2015**, *A71*, 3-8.

16. Sheldrick, G. M. Crystal Structure Refinement with SHELXL. *Acta Cryst*. **2015**, *C71*, 3-8.

17. Kasibhatla, S., Amarante-Mendes, G. P., Finucane, D., Brunner, T., Bossy-Wetzel, E., Green, D. R. Acridine Orange.Ethidium Bromide (AO/EB) Staining to Detect Apoptosos. *Cold Spring Harbor Protocols*, **2006**, doi:10.1101/pdb.prot4493.

18. https://www.leicabiosystems.com/knowledge-pathway/he-staining-overview-a-guide-to-best-practices/ (accessed 05/03/2020).

19. http://autodock.scripps.edu/resources/adt (accessed 02/15/2020).

20. Brooks, B. R., Bruccoleri, R. E., Olafson, B. D., States, D. J., Swaminathan, S., Karplus, M. A. CHARMM: A Program for Macromolecular Energy Minimization and Dynamics Calculations. *J. Comp. Chem*. **1983**, *4*(2), 187-217.

21. Zhang, D. W., Zhang, J. Z. H. Molecular fractionation with conjugate caps for full quantum mechanical calculation of protein–molecule interaction energy. *J. Chem. Phys*., **2003**, (119), 3599–3605.

22. Gordon, M. S., Fedorov, D. G., Pruitt, S. R., Slipchenko, L. V. Fragmentation Methods: A Route to Accurate Calculations on Large Systems. *Chem. Rev*. **2012**, *112*, 632-672.

23. Costa, R. F.; Feire, V. N., Cavada, B. S., Caetano, E. W. S.; Lima-Filho, J. L., Albuquerque, E.L. Explaining statin inhibition effectiveness of HMG-CoA reductase by quantum biochemistry computations. *Phys. Chem. Chem. Phys*. **2012**, *14*, 1389-1398.

24. Becke, A. D. Density-functional thermochemistry. II. The effect of the Perdew-Wang generalized-gradient correlation correction. *J. Chem. Phys*. **1992**, 97, 9173-9177 and references cited therein.